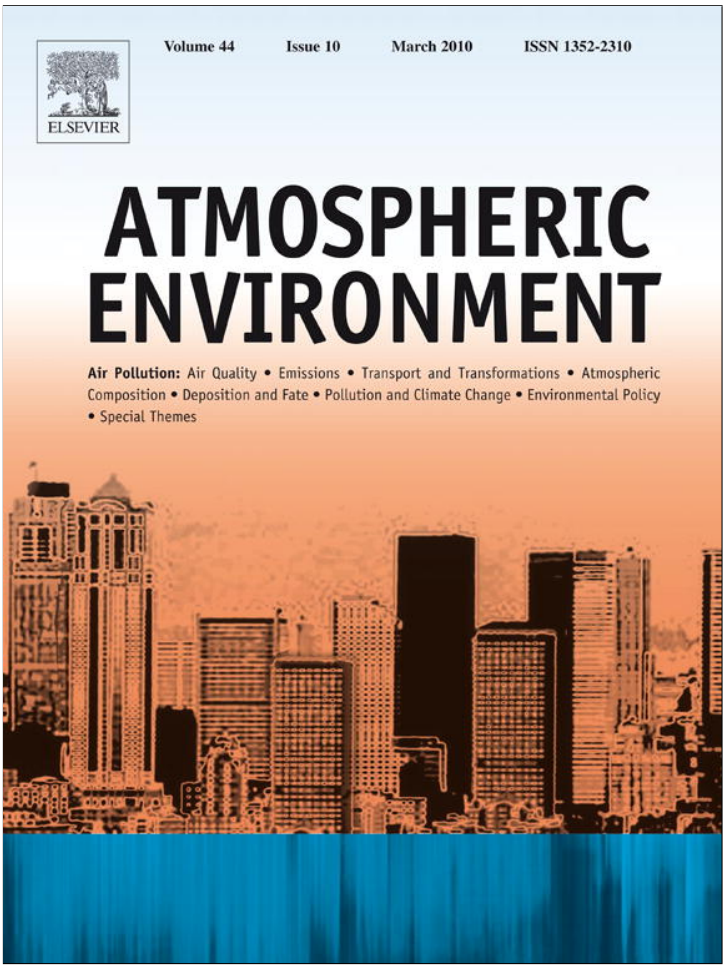

Atmospheric Environment 44 (2010) 1274–1283

Contents lists available at ScienceDirect

Atmospheric Environment

journal homepage: www.elsevier.com/locate/atmosenv

Satellite observations of the seasonal cycles of absorbing aerosols in Africa related to the monsoon rainfall, 1995–2008

M. de Graaf [a,*], L.G. Tilstra [a], I. Aben [b], P. Stammes [a]

[a] Royal Netherlands Meteorological Institute (KNMI), P.O. Box 201, 3730 AE De Bilt, The Netherlands
[b] Netherlands Institute for Space Research SRON, Sorbonnelaan 2, 3584 CA Utrecht, The Netherlands

ARTICLE INFO

Article history:
Received 22 July 2009
Received in revised form
21 December 2009
Accepted 23 December 2009

Keywords:
Absorbing aerosols
Remote sensing
African monsoon
Precipitation

ABSTRACT

The link between the African Monsoon systems and aerosol loading in Africa is studied using multi-year satellite observations of UV-absorbing aerosols and rain gauge measurements.

The main aerosol types occurring over Africa are desert dust and biomass burning aerosols, which are UV-absorbing. The abundance of these aerosols over Africa is characterised in this paper using residues and Absorbing Aerosol Index (AAI) data from Global Ozone Monitoring Experiment (GOME) on board ERS-2 and SCanning Imaging Absorption SpectroMeter for Atmospheric ChartograpHY (SCIAMACHY) on board Envisat.

Time series of regionally averaged residues from 1995 to 2008 show the seasonal variations of aerosols in Africa. Zonally averaged daily residues over Africa are related to monthly mean precipitation data and show monsoon-controlled atmospheric aerosol loadings. A distinction is made between the West African Monsoon (WAM) and the East African Monsoon (EAM), which have different dynamics, mainly due to the asymmetric distribution of land masses around the equator in the west. The seasonal variation of the aerosol distribution is clearly linked to the seasonal cycle of the monsoonal wet and dry periods in both studied areas.

The residue distribution over Africa shows two distinct modes, one associated with dry periods and one with wet periods. During dry periods the residue varies freely, due to aerosol emissions from deserts and biomass burning events. During wet periods the residue depends linearly on the amount of precipitation, due to scavenging of aerosols and the prevention of aerosol emissions from the wet surface. This is most clear over east Africa, where the sources and sinks of atmospheric aerosols are controlled directly by the local climate, i.e. monsoonal precipitation. Here, the wet mode has a mean residue of −1.4 and the dry mode has a mean residue of −0.3. During the wet modes a reduction of one residue unit for every 160 mm monthly averaged precipitation was found. Shielding effects due to cloud cover may also play a role in the reduction of the residue during wet periods.

A possible influence of aerosols on the monsoon, via aerosol direct and indirect effects, is plausible, but cannot directly be deduced from these data.

1. Introduction

Over Africa, two phenomena play dominant roles in the local weather and climate. Firstly, the monsoon is the driving mechanism of the climate on the continent, and therefore plays an important role in the social and economic development of the people in the tropics. Secondly, dust storms from the dry areas have a profound impact on the weather conditions and lives of the local people.

Scientifically, the first explanations of the monsoon were proposed in the seventeenth and eighteenth centuries by Halley and Hadley (see Webster, 1987). Since then an enormous amount of literature has been published describing the dynamics and controls of the African monsoon in ever more detail. Recently, the African Monsoon Multidisciplinary Analysis (AMMA) focused on the mutual interaction of the WAM system with the global climate, and on the impacts for the local population (Redelsperger et al., 2006).

Aerosols have become a scientific focus much more recently, particularly after aerosols were identified as the largest uncertainty in the modelling of climate radiative forcing (IPCC, 2001). Huge amounts of aerosols originate from deserts and vegetation fires on the African continent, which makes it one of the most interesting

* Corresponding author.
E-mail address: graafdem@knmi.nl (M. de Graaf).

1352-2310/$ – see front matter © 2010 Elsevier Ltd. All rights reserved.
doi:10.1016/j.atmosenv.2009.12.038

places to study the aerosol impact on the local and global climate. Since the monsoon is influenced globally through many teleconnections, like El Niño Southern Oscillation (ENSO), sea surface temperature anomalies and the North-Atlantic Oscillation (NOA), anomalies induced by aerosol loading fluctuation can potentially have global effects.

Aerosols are known to influence climate mainly through aerosol–cloud feedbacks. As cloud condensation nuclei (CCN), aerosols influence cloud formation and cloud albedo (Twomey, 1977), cloud lifetime (Albrecht, 1989), cloud height (Pincus and Baker, 1994) and precipitation, known as aerosol indirect effects. Furthermore, absorbing aerosols can heat the atmosphere locally, changing the lapse rate and vertical stability of the atmosphere, influencing cloud lifetime. This effect is known as the semi-direct effect (Ackerman et al., 2000). Considering the large amount of aerosols that originate on the African continent, aerosol effects may influence the African monsoon.

A strong influence of an absorbing aerosol haze on local monsoon dynamics was demonstrated in Asia. South Asia is an area with one of the highest semipermanent concentrations of anthropogenic absorbing aerosols, due to urbanisation and population growth (Lelieveld et al., 2001). The effects of the absorption of solar radiation by these aerosols on the tropospheric dynamics was studied extensively during the Indian Ocean Experiment (INDOEX) (Ramanathan et al., 2001) and subsequent observational (e.g. Lau and Kim, 2006; Bollasina et al., 2008) and modelling studies (e.g. Chung et al., 2002; Ramanathan and Ramana, 2005). These studies showed that a 3–km thick brownish haze layer over southeast Asia, the Indian Ocean and parts of the western Pacific perturbs the radiative energy budget in the region to induce anomalies in the Asian monsoon circulation and rainfall.

Over Africa, the main types of aerosols are desert dust and biomass burning aerosols. Several hundred million tons of desert dust from the Sahara are estimated to be transported to the tropical North-Atlantic Ocean and the Mediterranean Sea yearly (D'Almeida, 1986; Prospero et al., 1996; Engelstaedter et al., 2006). Especially the western Sahara is a major source for dust (e.g. Prospero et al., 2002; Reid et al., 2003; Kaufman et al., 2005) and the most important source for mineral aerosols globally. Desert dust affects the climate system in many ways. It absorbs solar radiation in the UV, provides surfaces for chemical reactions, and affects cloud nucleation and optical properties. The iron content in desert dust plays a major role in ocean fertilisation and oceanic carbon dioxide uptake, thereby affecting the global carbon budget (Gao et al., 2001). Dust transported to downwind terrestrial ecosystems can play a major role in soil formation and nutrient cycling (Okin, 2005). Dust production in the western Sahara peaks in June/July, when intense surface heating causes the InterTropical Convergence Zone (ITCZ) to reach its northern-most position. Dust production is controlled by small-scale high-wind events (Engelstaedter and Washington, 2007). In summer, north of the ITCZ at the InterTropical discontinuity (ITD), which is the interface between the monsoon and the Harmattan, near-surface turbulence and vertical winds peak, producing strong dust outbreaks. The mobilised dust can be transported vertically along the monsoon–Harmattan interface, due to the existence of mechanical shear above the monsoon layer. The dust thus becomes available for long-range transport by the Harmattan and is carried over the North-Atlantic Ocean (Bou Karam et al., 2008, 2009).

Smoke and other biomass burning aerosols are produced by annually recurring savanna fires in all vegetated parts of Africa, during the local dry period. Biomass burning aerosols are chemically very active and their internal chemical and physical properties change quickly during the first few hours to days after their creation (Reid et al., 2005). The cores of fresh biomass burning aerosols are made up of black carbon and other substances, depending on the source (e.g. combustion and fuel type). These aerosols absorb solar radiation over a broad range of the solar spectrum. Fresh biomass burning aerosols are known to burn away clouds due to their heating of the atmosphere. This can cause smoke aerosols to have a net heating effect at the surface, instead of a cooling effect (Hansen et al., 1997; Koren et al., 2004). As the biomass burning aerosols age and move away from the source the aerosols are coated with water, reducing the absorption efficiency of the black carbon core and the aerosols become very efficient CCN. Therefore, scenes with aged biomass burning aerosols, which are of much interest for global climate dynamics, are often cloud contaminated.

Aerosols are removed from the atmosphere by gravity or dynamic processes (dry deposition) or by incorporation in rain drops and subsequent precipitation (wet deposition). Aerosols can form cloud droplets and precipitate (in-cloud scavenging) or be incorporated in falling rain droplets (below-cloud scavenging). Dry deposition is important mainly for very large particles, which are quickly returned to the surface. In-cloud scavenging is more important than below-cloud scavenging for averaged-sized particles, since falling cloud droplets produce a flow field around the droplet which is followed by the particle, preventing scavenging. Below-cloud scavenging is important for very small particles (e.g. smoke) of which the Brownian motion exceeds the rain droplet fall velocity, and for coarse particles with large inertness (e.g. dust) (Henzing et al., 2006).

Clearly, the mechanisms of aerosol production and removal are inevitably linked to the monsoon on the African continent. In this paper we focus on a multi-year link between the African Monsoon, both the WAM and EAM, and the presence of UV-absorbing aerosols on a monthly timescale.

The presence of aerosols over Africa can be demonstrated using satellite observations. Satellite instruments are ideal for the monitoring of inhomogeneous daily aerosol distributions. However, most current satellite aerosol retrieval algorithms rely on cloud screening before retrieving aerosol information (e.g. Tanré et al., 1996; Veefkind et al., 2000; Diner et al., 2001; Martins et al., 2002; Hauser et al., 2005; Holzer-Popp et al., 2008). This means a huge reduction of the monitoring capability of satellite instruments, especially for those with large footprints. Furthermore, it prohibits remote sensing studies of rainfall–aerosol interactions in those cases where clouds are present.

An aerosol satellite product that does not rely on cloud screening is the residue, a quantity which compares the scene colour in the UV to that of a pure Rayleigh atmosphere (Herman et al., 1997; Torres et al., 1998; De Graaf et al., 2005). It can be used to indicate absorbing aerosols, even in the presence of clouds, for which it has been extensively used (e.g., Gleason et al., 1998; Tanré et al., 2001; Prospero et al., 2002; Duncan et al., 2003; Eckardt and Kuring, 2005; Kaufman et al., 2005; Fromm et al., 2006). In these cases it is often called the UV Absorbing Index (UVAI) or Absorbing Aerosol Index (AAI), both of which are a part of the residue, indicating absorption. In the UV most surface types are spectrally flat and the residue works equally well over both land and ocean surfaces. However, bare surfaces, e.g. deserts, can have a spectrally dependent surface albedo (Kleipool et al., 2008), causing spurious residues of up to 1. Similarly, ocean colour differences can cause residues shifts down to −1 (Torres et al., 1998).

The residue still suffers from cloud contamination, when clouds shield underlying aerosol layers from view. Such layers cannot be detected, since UV radiation often does not penetrate a cloud. Also thin clouds and scattering aerosols can produce small negative values of the residue (Penning de Vries et al., 2009), opposing the effect of aerosols in a scene. Furthermore, when UV-absorbing aerosols overlay a cloud, the residue is increased: for smoke, the

suppression of cloud multiple scattering due to aerosol absorption is more efficient in the UV, because of the decreasing Aerosol Optical Thickness (AOT) with wavelength, even if the refractive index of smoke aerosols is wavelength independent. For dust, the optical properties are wavelength dependent in the UV, which again suppresses the cloud multiple scattering more efficiently at smaller wavelength, increasing the residue (De Graaf et al., 2007). Residues with values smaller than 1, which amounts to a radiance difference of ±2.3%, are usually considered too small to distinguish geophysical signals from instrumental calibrations errors. Here, the results are compared to other information that is available in the literature when interpreting residues in terms of either desert dust or biomass burning aerosols.

The residue is available from Total Ozone Mapping Spectrometer (TOMS) data (Herman et al., 1997; Torres et al., 1998) from as early as 1978 to 1994 and 1996 to 2005, from GOME for the period 1995 to 2003 (De Graaf et al., 2005), from SCIAMACHY for the period 2002 to present (De Graaf and Stammes, 2005; Tilstra et al., 2007), and from Ozone Monitoring Instrument (OMI) for the period 2004 to present (Torres et al., 2007). In the current paper GOME residues from 1995 to 2000 and SCIAMACHY residues from 2002 to 2008 are used to indicate the presence of absorbing aerosols over Africa in those periods.

In this paper we investigate the effect of monsoonal cloud cover and precipitation on the residue in a statistical manner. Monsoon dynamics can be characterised by many parameters, but we focus on precipitation, since it is one of the most prominent features of a monsoonal weather system. Furthermore, wet deposition, or scavenging, is also the most important removal process of aerosols from the atmosphere. Global rain gauge observations are used to describe the precipitation. Satellite observations of precipitation are also available, but rain gauges have a long history in characterising synoptic weather systems, and using them avoids biases that can occur when comparing two satellite data records.

The paper is structured as follows: Section 2 introduces the instruments and the data used. In section 3 time series of the residue show the seasonal trends of desert dust and biomass burning aerosols in selected areas in Africa. These are compared to regionally and temporally averaged residue and precipitation data in monsoon-controlled areas. The observations are used to show the impact of the monsoon on aerosol abundance in Africa. Finally, conclusions are drawn in Section 4.

2. Methods and data

2.1. GOME instrument

GOME is a 4-channel grating spectrometer, operating in the wavelength range of 237–794 nm with a spectral resolution of 0.2–0.4 nm (Burrows et al., 1999). GOME was launched in April 1995 on board the ERS-2 satellite into a near-polar sun-synchronous orbit at a mean altitude of about 785 km, with a mean local equator crossing time of 10:30 LT. GOME performs nadir observations by scanning the surface from east to west (corresponding to a viewing zenith angle of −30° to +30°) in 4.5 s. One across-track scan is divided into three 1.5 s ground pixels with an average size of 40×320 km^2 each. Once per day the Sun is observed over a diffuser plate for radiometric calibration. Since 2000 GOME suffers from serious radiometric degradation in the UV.

2.2. SCIAMACHY instrument

SCIAMACHY is part of the payload of the European 'Environmental Satellite' Envisat, launched on 1 March 2002 into a near-polar sun-synchronous orbit at about 800 km altitude, with an equator crossing time of 10:00 LT for the descending node, orbiting the Earth every 100 min. SCIAMACHY is a spectrometer designed to measure sunlight, transmitted, reflected and scattered by the Earth's atmosphere or surface, in eight channels from 240 to 2380 nm at a spectral resolution of 0.2–1.5 nm (Bovensmann et al., 1999). The Earth radiance is observed in two alternating modes, nadir and limb, yielding data blocks called states. A state usually lasts about 65 s. The size of a nadir state is approximately 960×490 km^2. In nadir mode, SCIAMACHY scans the Earth from east to west in 4 s by rotating one of its internal mirrors. A state is divided into pixels of 60×30 km^2 for the largest part of the UV–visible channels. The extra-terrestrial solar spectral irradiance is measured each day, once per fourteen orbits.

From the spectral radiance and irradiance measurements the Earth's reflectance spectrum is determined. The reflectance is defined as $R_\lambda = \pi I_\lambda/(\mu_0 E_{0,\lambda})$, where I is the radiance at the top-of-atmosphere (TOA), E_0 is the solar irradiance at TOA perpendicular to the direction of the incident sunlight and μ_0 is the cosine of the solar zenith angle θ_0 at the surface.

2.3. Residue and the Absorbing Aerosol Index

Residues were computed from GOME and SCIAMACHY reflectances, using the same definition as for the TOMS Aerosol Index (Herman et al., 1997; Torres et al., 1998):

$$r_{\lambda,\lambda_0} = -100\left\{{}^{10}\log\left(\frac{R_\lambda}{R_{\lambda_0}}\right)^{\text{meas}} - {}^{10}\log\left(\frac{R_\lambda}{R_{\lambda_0}}\right)^{\text{Ray}}\right\}, \quad (1)$$

where r_{λ,λ_0} is the computed residue, R^{meas} are measured reflectances at wavelengths λ_0 and λ, and R^{Ray} are simulated clear sky (Rayleigh) reflectances for the same wavelengths and geometries as the measured reflectances. The residue is the difference between the measured reflectances and that of a pure Rayleigh scattering atmosphere, computed using a radiative transfer model assuming a molecular atmosphere and an ozone profile, bounded from below by a Lambertian surface with a freely adjustable albedo. Scattering effects are incorporated in the model atmosphere by varying the surface albedo. Ideally, only atmospheric absorption yields a difference between the modelled Rayleigh and real atmosphere, quantified by the positive part of the residue, often referred to as (Absorbing) Aerosol Index (AI or AAI). The largest absorbing effects in the atmosphere are caused by (UV-)absorbing aerosols when molecular (ozone) absorption is accounted for.

GOME reflectances R^{meas} at $\lambda = 335$ nm and $\lambda_0 = 380$ nm from 27 June 1995 to 31 December 2000 were used (De Graaf et al., 2005), and SCIAMACHY reflectances at $\lambda = 340$ nm and $\lambda_0 = 380$ nm from 1 August 2002 to 30 April 2008 (De Graaf and Stammes, 2005). The use of a different wavelength pair makes the GOME residue about 10% more sensitive to absorbing aerosols than the SCIAMACHY residue, which is corrected for in this study. The instrument degradation of GOME makes it currently unsuitable for residue retrievals beyond the year 2000. The degradation of SCIAMACHY is well monitored and corrected for in the residue. The data are available on a $1° \times 1.25°$ grid for each day, except for a few number of days with instrumental problems (Tilstra et al., 2007). The low temporal coverage of satellite observations is not so problematic, since aerosol residence times in the atmosphere are typically a few days.

2.4. Precipitation data

Precipitation data were obtained from the German Weather Service DWD (http://gpcc.dwd.de). These are quality-controlled

(automatic and manually) monitor data from 7000 to 8000 rain gauge stations. The data are available on a $1^\circ \times 1^\circ$ grid and monthly averaged. The two main error sources for rain gauge data are: (1) the systematic measurement error which results from evaporation out of the gauge and aerodynamic effects, when droplets or snow flakes are drifted by the wind across the gauge funnel, and (2) the stochastic sampling error due to a sparse network density (Schneider et al., 2008). An estimate for these errors is available only from 2007 onwards and therefore not applied. However, the first error is mainly large in cold seasons and snow areas and therefore not important here. The relative sampling error of gridded monthly precipitation is between 7 and 40% of the true area-mean if 5 rain gauges are used, and with 10 stations the error can be expected within the range of 5–20% (Rudolf et al., 1994). The error range for a given number of stations represents the spatial variability of precipitation in the considered region. The spatial distribution of the gauges in Africa is shown in Fig. 1. In this study only large spatial and temporal averages are used to account for the sparse network density and the low temporal coverage of residues. In spite of their low density, gauge measurements are better suited for monthly averaged precipitation measurements than satellite observations of rain, because of the low temporal coverage of satellite observations (typically once per day) and the strong diurnal cycle of monsoonal precipitation.

3. Results

3.1. Residue and precipitation for selected areas

Seven areas in and around Africa were selected, to study the local time series and trend of the residue from GOME and SCIAMACHY (see Fig. 1), 1: North-Atlantic Ocean (blue); 2: Northwest Africa (red); 3: Guinean zone (green); 4: South-Atlantic Ocean (cyan); 5: Northeast Africa (brown); 6: Central-east Africa (dark green); 7: Southern Africa (grey). The GOME residues were averaged over each of these areas daily from July 1995 to December 2000 and the SCIAMACHY residues from August 2002 to April 2008 (Fig. 2), to show the characteristic long-term time series of phenomena related to aerosols and clouds in these particular areas. The global daily mean residue was also determined. The global yearly mean residue is −1.2, for both GOME and SCIAMACHY (see bottom panel of Fig. 2). The GOME residue has a variation in the monthly mean of less than 0.25 and a small decreasing trend of −0.029 per year from 1995 to 2000. The trend is probably due to degradation of the GOME sensor; a residue difference of 0.029 amounts to a reflectance error of less than 0.07%. Between 2002 and 2008 the trend in global mean SCIAMACHY residue is removed due to degradation corrections. In individual cases positive residues are indicative for absorbing aerosol events. However, averaged values of the residue are indicative for absorbing events when the value is substantially higher than the global average of −1.2.

In Figs. 3 and 4 the zonally averaged GOME and SCIAMACHY residue of the boxed areas labelled 'WAM' and 'EAM' in Fig. 1 (30° S–30° N, 15° W–10° E) and (30° S–30° N, 15°–40° E) are compared to the zonally averaged precipitation in the same period and areas. The two areas correspond roughly to the WAM and EAM areas, which have different dynamics. East Africa is characterised by a continent that stretches to both sides of the equator. Furthermore, the EAM is influenced by the presence of large meridional mountain ranges and large inland lakes. The WAM on the other hand, is characterised by a strong contrast of a large continental area north of the equator and oceanic regions south of the equator (e.g. Webster, 1987; Janicot et al., 1998; McGregor and Niewold, 1998). However, the sparse distribution of rain gauges in the South-Atlantic Ocean must be considered when interpreting the precipitation data south of 10° S in Fig. 3. Figs. 3 and 4 show a strong correlation between the residue and precipitation, even though precipitation data are irregular and therefore monthly averaged, while the residues were plotted for each day that the data were available. Clearly, there is a strong relationship between the abundance of atmospheric aerosols and the position of the ITCZ and monsoonal rains over Africa, as detailed below.

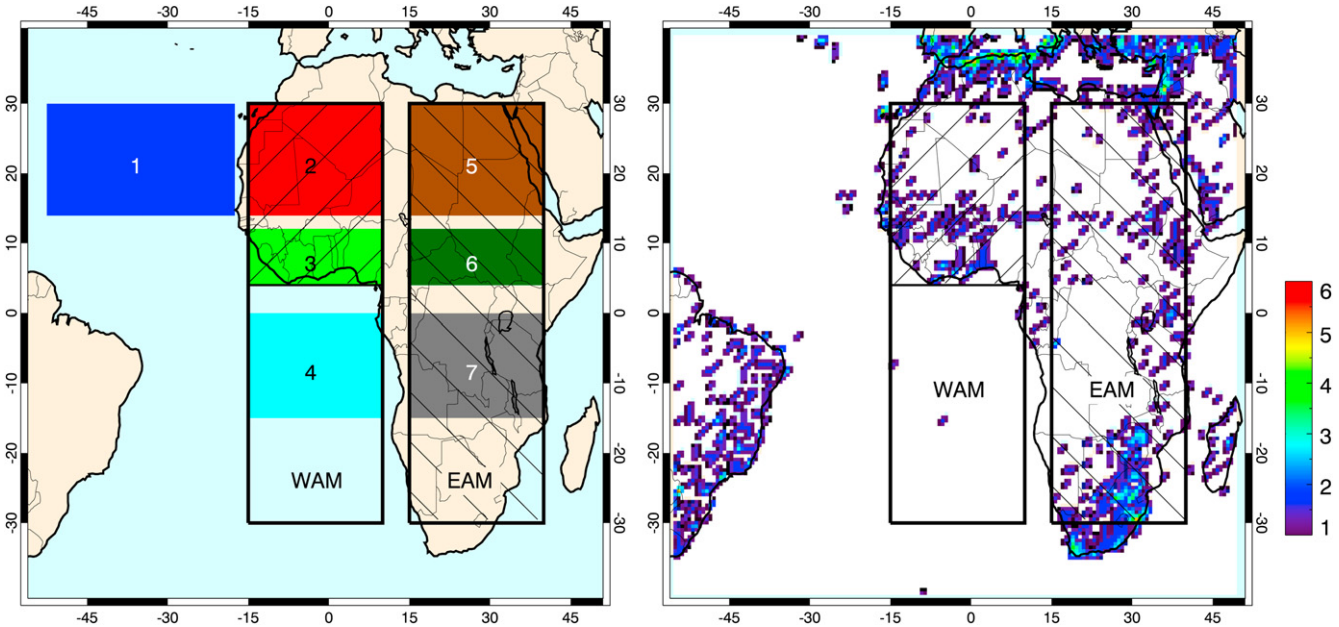

Fig. 1. Area under study. The left panel shows the coloured and numbered regions for which the area-averaged residue time series were determined from GOME and SCIAMACHY, as shown in Fig. 2. The shaded areas were defined as the West African Monsoon (WAM) area and the East African Monsoon (EAM) area. The temporal behaviour of the zonally averaged residue and precipitation for these areas are shown in Figs. 3 and 4, respectively. The right panel shows the number density of the rain gauges used in this paper.

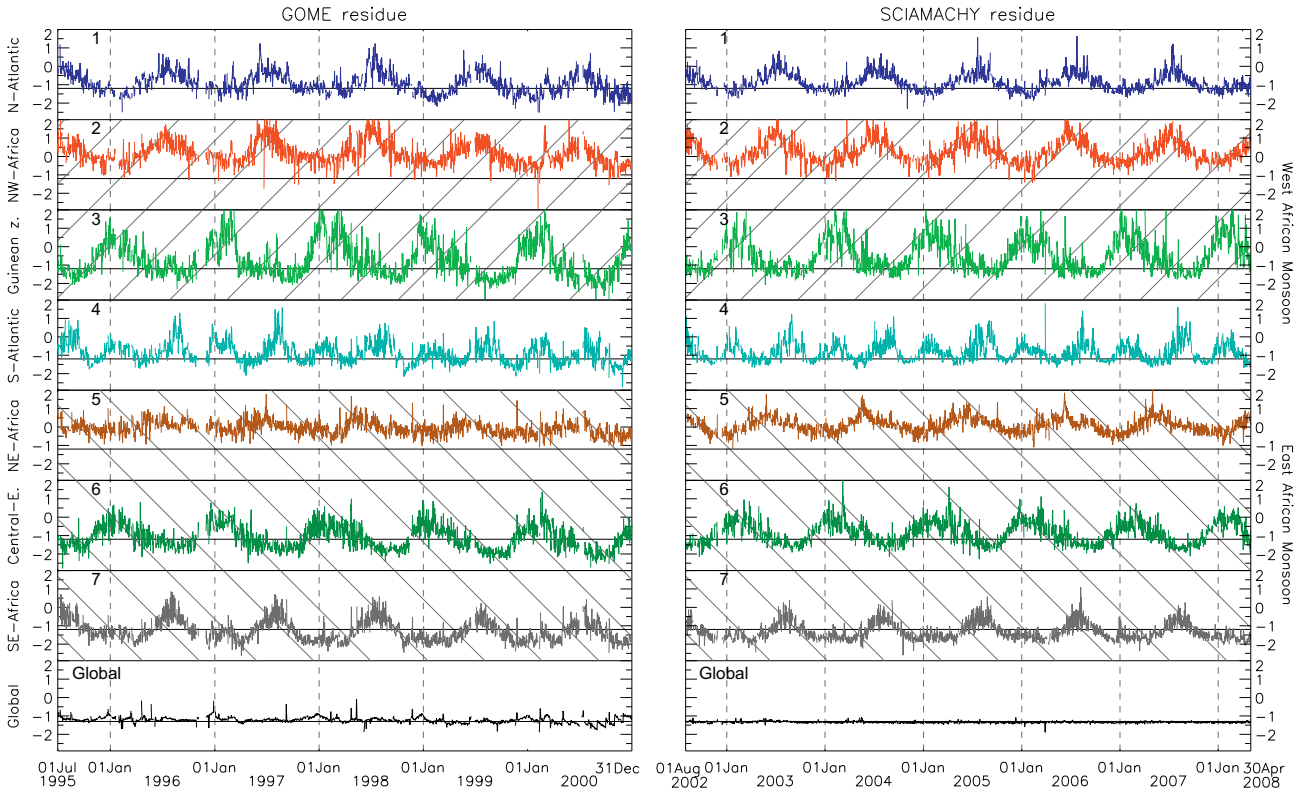

Fig. 2. Time series of the residue from GOME (July 1995–December 2000, left panel) and SCIAMACHY (August 2002–April 2008) in the areas indicated in Fig. 1. The solid black line in the bottom panel shows the global average.

3.2. West African monsoon–residue relationship

Over northwest Africa (area [2]) very high residues can be observed, with a strong seasonal variability (Fig. 2). In the western Sahara dust production peaks in June/July, which is reflected by the high residue in these months. The high correlation between the residue curves over northwest Africa and the North-Atlantic Ocean (area [1] in Fig. 2), confirms observations that dust over the North-Atlantic is mobilised in the western Sahara (e.g. Darwin, 1846).

In winter mean surface winds and the number of high-wind events decrease. The residue decreases accordingly. Dust production in winter in the Sahara is mainly associated with short-lived bursts of strong Harmattan winds (e.g. Evan et al., 2006; Engelstaedter and Washington, 2007).

Fig. 3 shows the same behaviour over the Sahara (north of 10° N), with high residue events in the boreal summer months, when the monsoon rains reach their northern-most position. This results in a very strong residue gradient from north to south. In the boreal winter months, or the dry period, the residue events are moderate and spread over a larger area.

This seasonal variation was also found using TOMS Aerosol Optical Thickness (AOT) (Torres et al., 2002), TOMS AI (Engelstaedter and Washington, 2007) and Meteosat Second Generation (MSG)-SEVIRI brightness temperature differences (BTD) dust index (Schepanski et al., 2007).

Over the Guinean zone, the region just north of the equator, a strong seasonal variation can be observed in the residue (area [3] in Fig. 2), out of phase with the residue signal in the Sahara and North-Atlantic. Fig. 3 shows that this seasonal variation of residue is highly correlated with the seasonal variation of the monsoonal rains, with increasing precipitation decreasing the residue. The wet season is during the summer months for this area, when the ITCZ reaches its northern–most position and aerosols are mostly absent. The dry season is during the winter months, when absorbing aerosols can originate from local savanna burning events or from desert dust blown south from the Sahara (e.g. Mallet et al., 2006). From the GOME or SCIAMACHY residue itself no distinction can be made between the types or sources of the observed absorbing aerosols.

South of the equator primary maxima in residues in June/July and secondary maxima in December/January can be observed (area [4] in Fig. 2). This area experiences two wet (Oct.–mid Dec. and late Feb.–May) and two dry periods (Jun.–Sep. and Dec., Jan.) per year, as can be seen from Fig. 3, and during both dry periods high residues can be observed. The primary maxima are caused by anthropogenic biomass burning, of which the aerosol plumes extend over the South-Atlantic Ocean. North of the equator the monsoon rains form an effective boundary for aerosols in these months and no mixing of desert dust from the Sahara and local biomass burning aerosols occurs. During the secondary maxima however, the monsoonal rains are located south of this area and the residue is comprised of local biomass burning aerosols, mixed with desert dust and biomass burning aerosols originating in the Sahel and the Sahara. Secondary maxima were also found in TOMS residues in a box just south of the equator in Africa between 1984 and 1988 (Herman et al., 1997) and less clearly in TOMS AOT from 1978 to 1993 (Torres et al., 2002), because in the latter only data from 5°– to 25° S was used. These secondary maxima were attributed to excursions of smoke aerosols from events just north of the equator to the south by the prevailing winds. However, since the origins of absorbing aerosols north of the equator are uncertain, the biomass burning aerosols in these secondary maxima may also be mixed with desert dust.

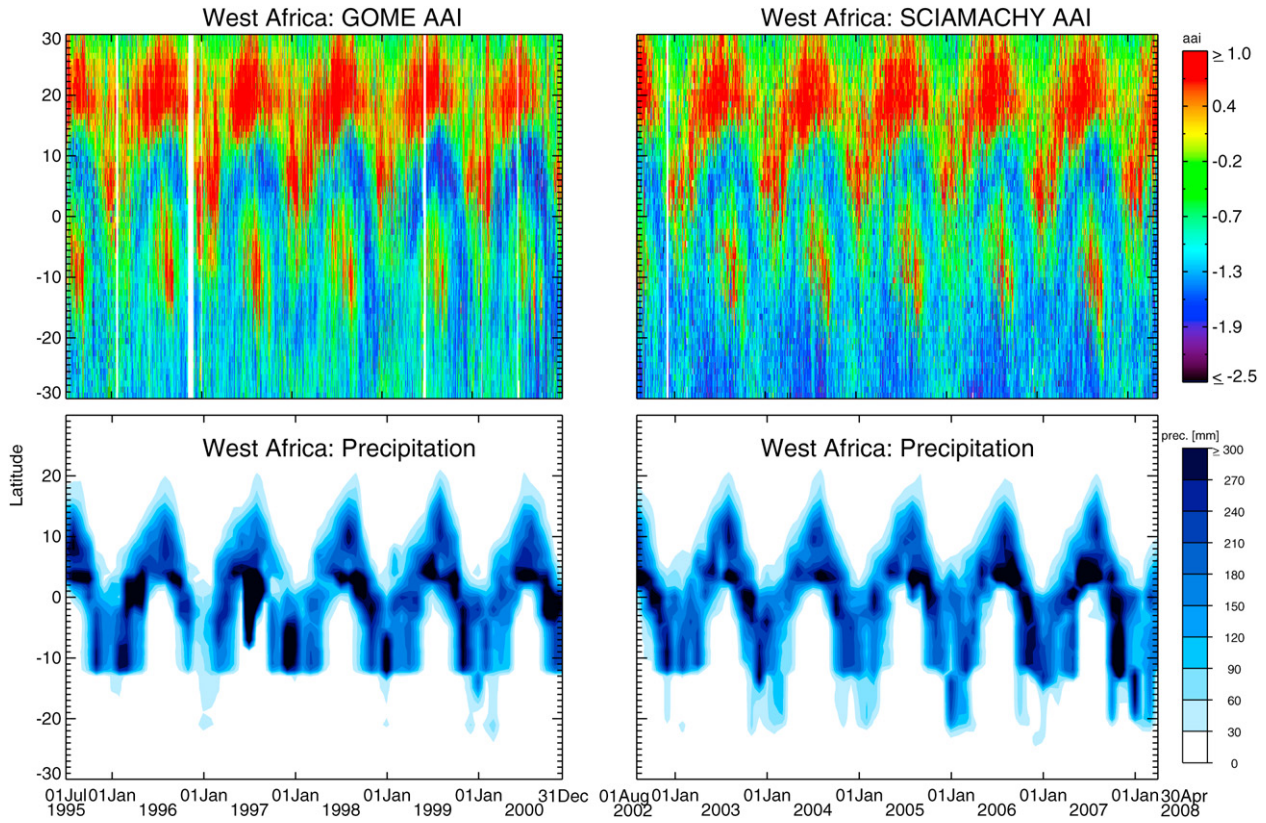

Fig. 3. Zonally averaged residue for each day between July 1995 and December 2000 (left top panel) and August 2002–April 2008 (right top panel) as a function of latitude in West Africa, and the 1° × 1° gridded and monthly averaged GPCC precipitation, averaged zonally, in the same area and same periods (lower panels).

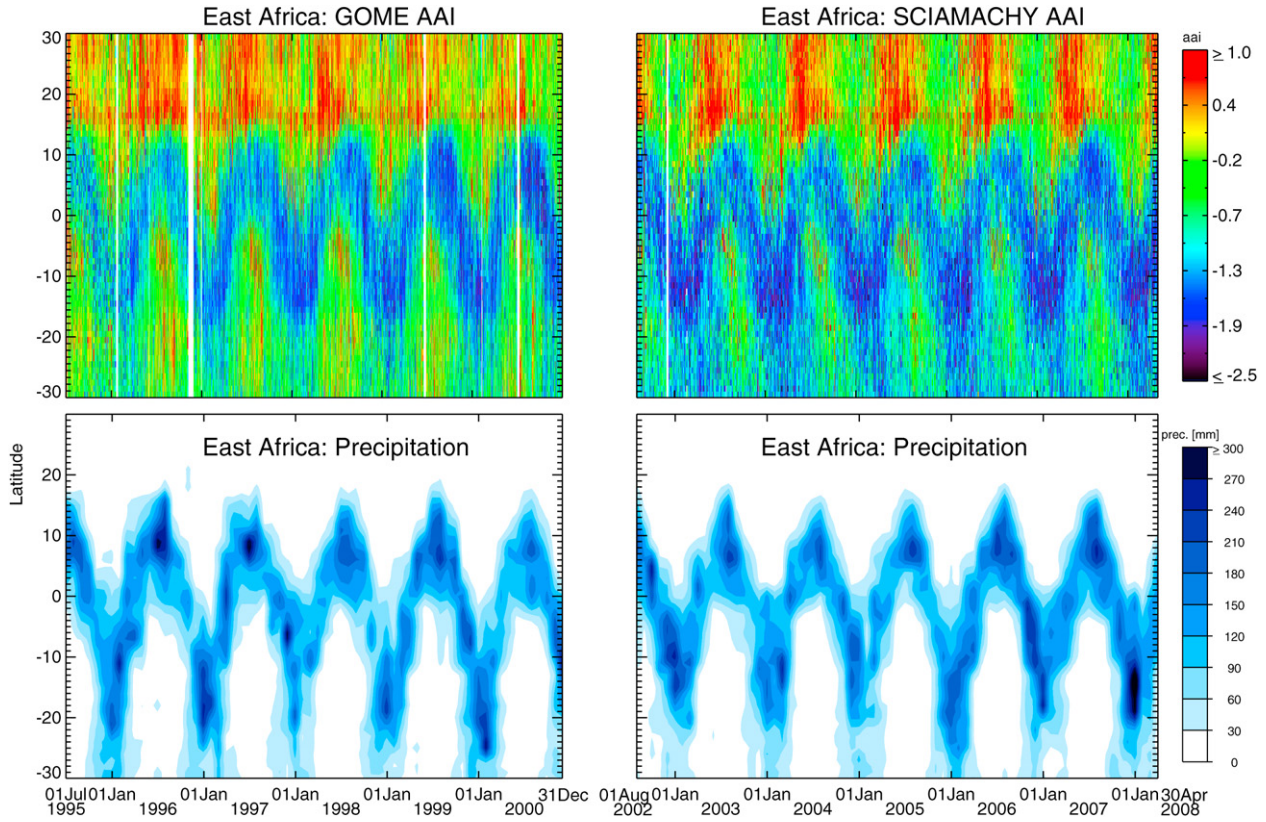

Fig. 4. Same as Fig. 3 but for East Africa (see shaded areas in Fig. 1.)

3.3. East African monsoon–residue relationship

In northeast Africa (area [5], Fig. 2) the average residue is high, but the seasonal variation is small compared to northwest Africa, especially in the GOME data. The SCIAMACHY data show less noise and the seasonal variation is more clear, but still smaller than in western Africa. Fig. 4 shows that north of 10° N the average residues are smaller than in the west, both during the wet and the dry seasons. However, this region includes the Bodélé depression, an area centred around 17° N, 18° E, which is known to be a major source of desert dust aerosols year-round (Prospero et al., 2002; Washington et al., 2006; Todd et al., 2007). The effect of this permanent dust source can be seen as continuous line of high residue year-round at 17° N.

Central-east Africa (area [6], Fig. 2) shows residues out of phase compared to the rest of the continent, similar to the Guinean zone lying to the west, although with smaller amplitude than the Guinean area. Like this region, Central-east Africa experiences low (high) aerosol loading during wet (dry) periods.

Southeast Africa (area [7], Fig. 2) also shows alternating high and low residues. The high values are mainly local biomass burning aerosols during the local dry season, which are absent during the local wet season (e.g. Stein et al., 2003). They are in phase with the desert dust production north of the northern-most position of the ITCZ (i.e. the eastern Sahara). No clear secondary maxima are present in this area.

Fig. 4 shows the asymmetry of the African Monsoon: in the boreal summer months a strong meridional gradient in precipitation, and residue, at around 15° N marks the northern boundary of the African Monsoon. This gradient is caused by the convergence of north-easterly flows from the southern Sahara and cool moist south-westerly monsoonal flows. The hot dry north-easterly continental air is less dense than the cool moist monsoonal flow and uplifted, capping the leading edge of the monsoonal flow and suppressing precipitation in the vicinity of the convergence zone. North of this zone the southern Sahara remains under the influence of subsiding north-easterly flows and is generally cloud-free, while south of the convergence zone cloud development and precipitation reaches its maximum (McGregor and Niewold, 1998). In southern Africa, at the southern-most position of the ITCZ this gradient is absent, due to the absence of large continental areas.

3.4. Residue wet and dry modes

The strong correlation between the residue and precipitation is confirmed by a more statistical analysis, as shown in Fig. 5. The left panels in this figure refer to the shaded areas of West Africa in Fig. 1 and the right panels to the shaded areas of East Africa, which means that oceanic areas were excluded. The monthly averaged precipitation data were regridded to match the 1° × 1.25° residue data grid and plotted as a function of the monthly averaged residue data (grey data points in Fig. 5a and b), for all available data between

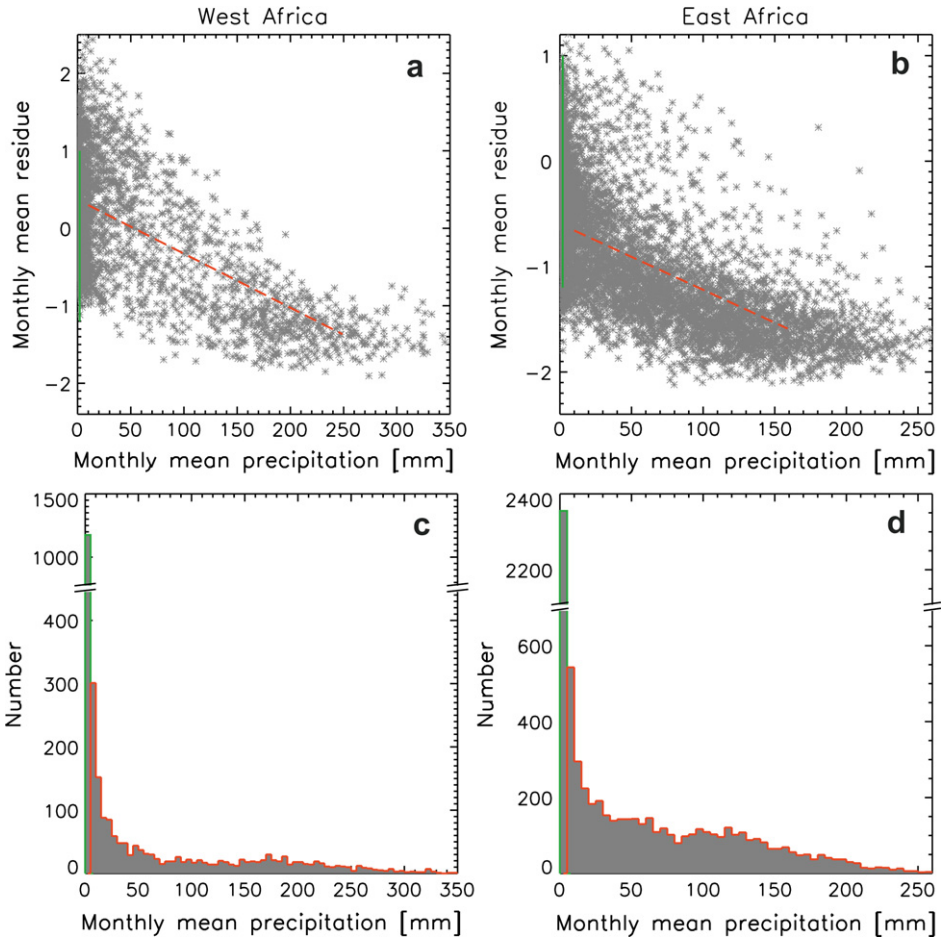

Fig. 5. Monthly averaged residue as a function of the monthly averaged precipitation, between 1995 and 2008, in (a) West Africa and (b) East Africa; And total number of the monthly mean precipitation in (c) West Africa and (d) East Africa. Note that the *y*-axes are cut: the total number of non-precipitation events is about half of the precipitation events in East Africa and 2/3 in West Africa. The green solid lines indicate data associated with no precipitation, and the red dashed lines indicate data associated with precipitation. (For interpretation of the references to colour in this figure legend, the reader is referred to the web version of this article.)

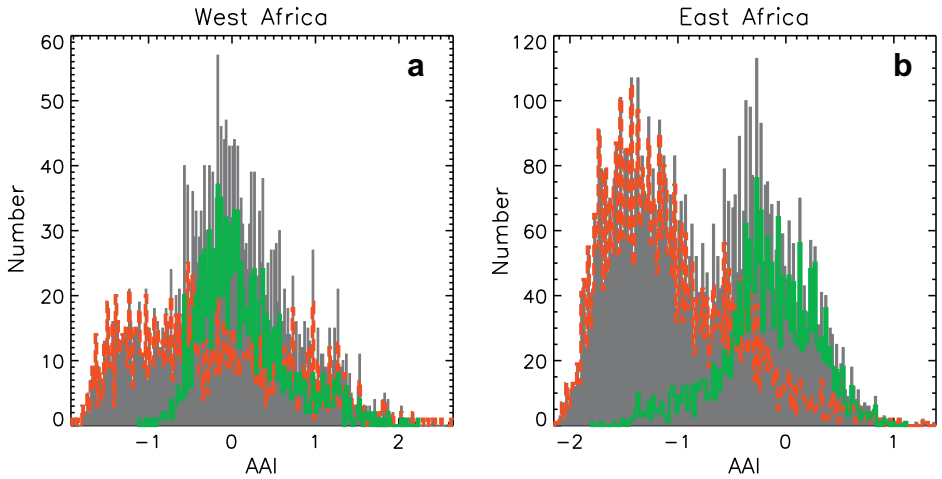

Fig. 6. Frequency distribution of residue in (a) West Africa and (b) East Africa in grey. The green solid lines indicate the 'dry' mode data, associated with no precipitation, and the red dashed lines indicate the 'wet' mode data, associated with precipitation. The red and green histograms add up to the total number of events plotted in grey. (For interpretation of the references to colour in this figure legend, the reader is referred to the web version of this article.)

1995 and 2008. The green solid lines indicate the data that correspond to regions and months without precipitation, i.e. less than 5 mm precipitation in a month, while the red dashed lines correspond to data with more than 5 mm precipitation in a month, as shown in Fig. 5c and d.

Fig. 5c and d shows the nature of precipitation data, which is irregular and sparse and non-normally distributed. There are many regions with months of no precipitation, and a long tail of regions and months with precipitation. Note that the *y*-axes of the graphs are cut to enlarge the tails of the distributions; the ratio of dry and wet events is about 1:2 in East Africa and 2:3 in West Africa.

When there is no precipitation the residue can have any value above about −1.5, which seems to be its monthly mean minimum in dry periods (Fig. 5a and b). In other words, during dry periods any amount of absorbing aerosols can be found in the atmosphere. These data associated with no precipitation are indicated by the green lines.

During precipitation periods there appears to be a relation between the residue and the amount of precipitation. A linear regression, $\bar{r} = a_0 + a_1\bar{p}$, where $\bar{r}$ is the monthly mean residue and $\bar{p}$ is the monthly mean precipitation, showed a relation of $a_0 = 0.04$ and $a_1 = -0.007$ mm^{-1} in West Africa, and $a_0 = -0.6$ and $a_1 = -0.006$ mm^{-1} in East Africa, indicated by the red dashed lines. The slope may be larger, since the residue seems to have a lower limit around −2 (East Africa), independent of (heavy) precipitation. The low average residues during the wet periods may be caused by scavenging of aerosols by monsoonal rains, heavy cloud cover during precipitation events shielding aerosols from view and the prevention of aerosol emissions due to wetting of the surface.

The residue data show two modes of frequency (grey histograms in Fig. 6). The overlaid red, dashed (precipitation) and green, solid (non-precipitation) histograms show that these peaks are associated with wet and dry periods, respectively. This is especially clear in East Africa, where the sources (desert storms and vegetation burning on land) and sinks (scavenging by rain) of aerosols are close together. The modes in East Africa have a mean around −1.4 and one around −0.3. In West Africa the two peaks are less distinct, but the red and green histograms still show that the residue behaves differently in wet conditions and in dry conditions. This has not formerly been investigated, since residues are usually only considered when positive and associated with absorbing effects.

4. Discussion and conclusions

The presence of desert dust and biomass burning aerosols in Africa is detected using GOME and SCIAMACHY residue data from 1995 to 2008. Residue data can be used for the daily monitoring of these UV-absorbing aerosols in monsoon areas. Both aerosol types are abundant over the African continent and the surrounding oceans, and both experience seasonal cycles in their distributions. The seasonal cycles are influenced by the geographic location of their sources and the prevailing meteorological conditions. The latter is dominantly controlled by the African Monsoon, which is reflected in the relationship between the residue and precipitation.

The relationship between the aerosol abundance in Africa and the African monsoon is shown based on the correlation between monthly averaged precipitation and residue data during wet periods over continental areas. The residue over Africa has two distinct modes, of which only the 'dry' mode has been studied so far. During the 'wet' mode, the correlation showed a reduction of residue by 1 for every 160 mm monthly averaged precipitation in East Africa, until it reached a lower limit of −2. The correlation shows that negative residues also contains information on precipitation, as it does on clouds and scattering aerosols (Penning de Vries et al., 2009).

The two modes of the residue shown in Fig. 6 have not been presented before. Globally the residue is more or less normally distributed with a mean of −1.2 (not shown). In East Africa, the dry mode mean of the residue is −0.3, and the wet mode mean is −1.4. The modes are less distinct over West Africa. The high value of the residue during the dry mode is the result of desert dust and biomass burning aerosol emissions. The most likely cause of the lowering of the residue during the wet mode is scavenging of aerosols during precipitation events. Also, wetting of the surface may prevent emissions of aerosols after precipitation events, which will be reflected in the monthly mean residue. Furthermore, aerosol layers may be shielded from (satellite) view by cloud cover. However, monsoonal precipitating cloud systems are often convective cumulus systems reaching all the way to the tropopause, while shielding will be more important in cases of stratus clouds. Clouds themselves can yield negative residues, especially when a scene is partially covered with clouds (Penning de Vries et al., 2009), which is often the case with the large footprints of GOME and SCIAMACHY. In view of a recent discussion about reduced TOMS AI during precipitation events over west Africa

(Williams, 2008; Engelstaedter and Washington, 2008), we note that the data used here are too coarse in both spatial and temporal sense to draw definitive conclusions about the causes of this relationship. A more detailed study will be required to resolve this issue.

The separation of modes over the EAM area is stronger than over the WAM area. Apparently, the emission to and removal from the atmosphere of aerosols are more directly influenced by the local climate (monsoonal precipitation) over the EAM area than over the WAM area. The EAM is characterised by a strong influence of the local geography and morphology on the monsoon system, which is reflected in the aerosol loading. On the other hand, the WAM area aerosol loading is determined more by air masses advected from either the Sahara or the clean Atlantic Ocean. Although local precipitation and cloud cover clearly have an influence on the residue, large scale effects determine the sign and distribution of the residue over the WAM area.

The enormous amount of aerosols that originate from Africa justify a thorough investigation of cloud–aerosol and rainfall feedbacks on this continent, since aerosol loading can have a profound impact on cloud forming and atmospheric stability and circulation. An example is the existence of clouds polluted by biomass burning over the South–Atlantic west of Africa (De Graaf et al., 2007). These aerosols were found to act both as CCN and absorb solar radiation in and above the clouds. These opposing effects influence cloud formation and cloud lifetime and will in turn have an impact on the strength and location of the African monsoon. However, from the current study no conclusions can be drawn about indirect effects of the investigated aerosols, since both aerosol abundance and rainfall may be simultaneously influenced by other dynamic affects, but the aerosol–monsoon relationship is worth a more detailed investigation.

References

Ackerman, A.S., Toon, O.B., Stevens, D.E., Heymsfield, A.J., Ramanathan, V., Welton, E.J., 2000. Reduction of tropical cloudiness by soot. Science 288, 1042–1047. doi:10.1126/science.288.5468.1042.

Albrecht, B., 1989. Aerosols, cloud microphysics, and fractional cloudiness. Science 245, 1227–1230.

Bollasina, M., Nigam, S., Lau, K.-M., 2008. Absorbing aerosols and summer monsoon evolution over South Asia: an observational portrayal. J. Clim. 21, 3221–3239. doi:10.1175/2007JCLI2094.1.

Bou Karam, D., Flamant, C., Knippertz, P., Reitebuch, O., Pelon, J., Chong, M., Dabas, A., 2008. Dust emissions over the Sahel associated with the West African monsoon intertropical discontinuity region: a representative case-study. Q.J.R. Meteorol. Soc. 134, 621–634. doi:10.1002/qj.244.

Bou Karam, D., Flamant, C., Tulet, P., Chaboureau, J.-P., Dabas, A., Todd, M.C., 2009. Estimate of Sahelian dust emissions in the intertropical discontinuity region of the West African Monsoon. J. Geophys. Res. 114 (D13106). doi:10.1029/2008JD011444.

Bovensmann, H., Burrows, J.P., Buchwitz, M., Frerick, J., Noël, S., Rozanov, V.V., Chance, K.V., Goede, A.P.H., 1999. SCIAMACHY: mission objectives and measurement modes. J. Atmos. Sci. 56 (2), 127–150. doi:10.1175/1520-0469.

Burrows, J.P., et al., 1999. The global ozone monitoring experiment (GOME): mission concept and first scientific results. J. Atmos. Sci. 56 (2), 151–175. doi:10.1175/1520-0469.

Chung, C., Nigam, S., Kiehl, J.T., 2002. Effects of the South Arabian absorbing haze on the northeast monsoon and surface-air heat exchange. J. Clim. 15, 2462–2476.

D'Almeida, G.A., 1986. A model for Saharan dust transport. J. Clim. Appl. Meteorol. 24, 903–916.

Darwin, C., 1846. An account of the fine dust which often falls on vessels in the Atlantic Ocean. Q.J. Geol. Soc. 1–2, 26–30. doi:10.1144/GSL.JGS.1846.002.01-02.09.

De Graaf, M., Stammes, P., 2005. SCIAMACHY absorbing aerosol index. Calibration issues and global results from 2002–2004. Atmos. Chem. Phys. 5, 3367–3389.

De Graaf, M., Stammes, P., Torres, O., Koelemeijer, R.B.A., 2005. Absorbing aerosol index: sensitivity analysis, application to GOME and comparison with TOMS. J. Geophys. Res. 110, D01201. doi:10.1029/2004JD005178.

De Graaf, M., Stammes, P., Aben, E.A.A., 2007. Analysis of reflectance spectra of UV-absorbing aerosol scenes measured by SCIAMACHY. J. Geophys. Res. 112, D02206. doi:10.1029/2006JD007249.

Diner, D.J., et al., 2001. MISR aerosol optical depth retrievals over Southern Africa during the SAFARI-2000 dry season campaign. Geophys. Res. Lett. 28 (6), 3127–3130. doi:10.1029/2001GL013188.

Duncan, B.N., Bey, I., Chin, M., Mickley, L.J., Fairlie, T.D., Martin, R.V., 2003. Indonesian wildfires of 1997: impact on tropospheric chemistry. J. Geophys. Res. 108 (D15), D154458. doi:10.1029/2002JD003195.

Eckardt, F.D., Kuring, N., 2005. SeaWiFS identifies dust sources in the Namib Desert. Int. J. Remote Sens. 26 (19), 4159–4167. doi:10.1080/01431160500113112.

Engelstaedter, S., Washington, R., 2007. Atmospheric controls on the annual cycle of North African dust. J. Geophys. Res. 112, D03103. doi:10.1029/2006JD007195.

Engelstaedter, S., Washington, R., 2008. Reply to comment by E. Williams on "Atmospheric controls on the annual cycle of North African dust". J. Geophys. Res. 113, D23110. doi:10.1029/2008JD010275.

Engelstaedter, S., Tegen, I., Washington, R., 2006. North African dust emissions and transport. Earth Sci. Rev. 79 (1–2), 73–100. doi:10.1016/j.earscirev.2006.06.004.

Evan, A.T., Heidinger, A.K., Knippertz, P., 2006. Analysis of winter dust activity off the coast of West Africa using a new 24-year over-water advanced very high resolution radiometer satellite dust climatology. J. Geophys. Res. 111, D12210. doi:10.1029/2005JD006336.

Fromm, M., Tupper, A., Rosenfeld, D., Servranckx, R., McRae, R., 2006. Violent pyro-convective storm devastates Australia's capital and pollutes the stratosphere. Geophys. Res. Lett. 33 (L05815). doi:10.1029/2005GL025161.

Gao, Y., Kaufman, Y.J., Tanré, D., Kolber, D., Falkowski, P.G., 2001. Seasonal distributions of Aeolian iron fluxes to the global ocean. Geophys. Res. Lett. 28, 1. doi:10.1029/2000GL011926.

Gleason, J.F., Hsu, N.C., Torres, O., 1998. Biomass burning smoke measured using backscattered ultraviolet radiation: SCAR-B and Brazilian smoke interannual variability. J. Geophys. Res. 103, D24. doi:10.1029/98JD00160.

Hansen, J., Sato, M., Lacis, A., Ruedy, R., 1997. The missing climate forcing. Phil. Trans. R. Soc. Lond. B 352, 231–240.

Hauser, A., Oesch, D., Foppa, N., Wunderle, S., 2005. NOAA AVHRR derived aerosol optical depth over land. J. Geophys. Res. 110, D08204. doi:10.1029/2004JD005439.

Henzing, J.S., Olivié, D.J.L., van Velthoven, P.F.J., 2006. A parameterization of size resolved below cloud scavenging of aerosols by rain. Atmos. Chem. Phys. 6, 3363–3375.

Herman, J.R., Bhartia, P.K., Torres, O., Hsu, C., Seftor, C., Celarier, E.A., 1997. Global distributions of UV-absorbing aerosols from NIMBUS 7/TOMS data. J. Geophys. Res. 102, D14. doi:10.1029/96JD03680.

Holzer-Popp, T., Schroedter-Homscheidt, M., Breitkreuz, H., Martynenko, D., Klser, L., 2008. Improvements of synergetic aerosol retrieval for envisat. Atmos. Chem. Phys. 8 (24), 7651–7672.

IPCC, 2001. Climate Change 2001, The Scientific Basis. Cambridge University Press, Cambridge, 295 pp.

Janicot, S., Harzallah, A., Fontaine, B., Moron, V., 1998. West African monsoon dynamins and eastern equatorial Atlantic and Pacific SST anomalies. J. Clim. 11, 1874–1882.

Kaufman, Y.J., Koren, I., Remer, L.A., Tanré, D., Ginoux, P., Fan, S., 2005. Dust transport and deposition observed from the Terra-Moderate Resolution Imaging Spectroradiometer (MODIS) spacecraft over the Atlantic Ocean. J. Geophys. Res. 110, D10S12. doi:10.1029/2003JD004436.

Kleipool, Q.L., Dobber, M.R., de Haan, J.F., Levelt, P.F., 2008. Earth surface reflectance climatology from 3 years of OMI data. J. Geophys. Res. 113 (D18308). doi:10.1029/2008JD010290.

Koren, I., Kaufman, Y.J., Remer, L.A., Martins, J.V., 2004. Measurement of the effect of biomass burning aerosol on inhibition of cloud formation over the Amazon. Science 303, 1342–1345. doi:10.1126/science.1089424.

Lau, K.-M., Kim, K.-M., 2006. Observational relationships between aerosol and Asian monsoon rainfall, and circulation. Geophys. Res. Lett. 33 (L21810). doi:10.1029/2006GL027546.

Lelieveld, J., et al., 2001. The Indian Ocean experiment: widespread air pollution from South and Southeast Asia. Science 291 (5506). doi:10.1126/science.1057103.

Mallet, M., et al., 2006. Aerosol direct radiative forcing over Djougou (northern Benin) during the African Monsoon Multidisciplinary Analysis dry season experiment (Special Observation Period-0). J. Geophys. Res. 113 (D00C01). doi:10.1029/2007JD009419.

Martins, J.V., Tanré, D., Remer, L., Kaufman, Y., Mattoo, S., Levy, R., 2002. Modis Cloud screening for remote sensing of aerosols over oceans using spatial variability. Geophys. Res. Lett. 29 (12), 8009. doi:10.1029/2001GL013252.

McGregor, G.R., Niewold, S., 1998. Tropical Climatology, An Introduction to the Climates of the Low Latitudes. John Wiley & Sons, 352 pp.

Okin, G.S., 2005. Dependence of wind erosion and dust emission on surface heterogeneity: stochastic modeling. J. Geophys. Res. 110, D11208. doi:10.1029/2004JD005288.

Penning de Vries, M., Beirle, S., Wagner, T., 2009. UV aerosol indices from SCIAMACHY: introducing the SCattering Index (SCI). Atmos. Chem. Phys. Discuss. 9, 13569–13592.

Pincus, R., Baker, M.B., 1994. Effect of precipitation on the albedo susceptibility of clouds in the marine boundary layer. Nature 372, 250–252. doi:10.1038/372250a0.

Prospero, J.M., Barrett, K., Church, T., Dentener, F., Duce, R.A., Galloway, H., Levy II, H., Moody, J., Quinn, P., 1996. Atmospheric deposition of nutrients to the North Atlantic basin. Biogeochemistry 35, 27–73.

Prospero, J.M., Ginoux, P., Torres, O., Nicholson, S.E., Gill, T.E., 2002. Environmental characterization of global sources of atmospheric soil dust identified with the Nimbus 7 Total Ozone Mapping Spectrometer (TOMS) absorbing aerosol product. Rev. Geophys. 40 (1), 1002. doi:10.1029/2000RG000095.

Ramanathan, V., Ramana, M., 2005. Persistent, widespread, and strongly absorbing haze over the Himalayan foothills and the Indo-Gangetic Plains. Pure Appl. Geophys. 162, 1609–1626.

Ramanathan, V., et al., 2001. Indian Ocean Experiment: an integrated analysis of the climate forcing and effects of the great Indo-Asian haze. J. Geophys. Res. 106 (D22), 28371–28398.

Redelsperger, J.-L., Thorncroft, C.D., Diedhiou, A., Lebel, T., Parker, D.J., Polcher, J., 2006. African monsoon multidisciplinary analysis, an international research project and field campaign. Bull. Am. Meteorol. Soc. 87, 1739–1746. doi:10.1175/BAMS-87-12-1739.

Reid, J.S., Kinney, J.E., Westphal, D.L., et al., 2003. Analysis of measurements of Saharan dust by airborne and ground-based remote sensing methods during the Puerto Rico Dust Experiment (PRIDE). J. Geophys. Res. 108, D19. doi:10.1029/2002JD002493.

Reid, J.S., Koppmann, R., Eck, T.F., Eleuterio, D.P., 2005. A review of biomass burning emissions part II: intensive physical properties of biomass burning particles. Atmos. Chem. Phys. 5.

Rudolf, B., Hauschild, H., Rueth, W., Schneider, U., 1994. Terrestrial precipitation analysis: operational method and required density of point measurements. In: Desbois, M., Desalmond, F. (Eds.), Global Precipitations and Climate Change. NATO ASI Series I, vol. 26. Springer-Verlag, pp. 173–186.

Schepanski, K., Tegen, I., Laurent, B., Heinold, B., Macke, A., 2007. A new Saharan dust source activation frequency map derived from MSG-SEVIRI IR-channels. Geophys. Res. Lett. 34, L18803. doi:10.1029/2007GL030168.

Schneider, U., Fuchs, T., Meyer-Christoffer, A., Rudolf, B., 2008. Global Precipitation Analysis Products of the GPCC. Global Precipitation Climatology Centre (GPCC). Tech. Rep.. Deutscher Wetterdienst, Offenbach a.M.

Stein, D.C., Swap, R.J., Greco, S., Piketh, S.J., Macko, S.A., Doddridge, B.G., Elias, T., Bruintjes, R.T., 2003. Haze layer characterization and associated meteorological controls along the eastern coastal region of southern Africa. J. Geophys. Res. 108, D13. doi:10.1029/2002JD003237.

Tanré, D., Herman, M., Kaufman, Y.J., 1996. Information on aerosol size distribution contained in solar reflected spectral radiances. J. Geophys. Res. 101, D14. doi:10.1029/96JD00333.

Tanré, D., Bréon, F.M., Deuzé, J.-L., Herman, M., Goloub, P., Nadal, F., Marchand, A., 2001. Global observation of anthropogenic aerosols from satellite. Geophys. Res. Lett. 28, 24. doi:10.1029/2001GL013036.

Tilstra, L.G., de Graaf, M., Aben, I., Stammes, P., 2007. Analysis of 5 years SCIAMACHY Absorbing Aerosol Index data. In: Proceedings of the 2007 Envisat Symposium, ESA Special publication SP-636.

Todd, M.C., Washington, R., Martins, J.V., Dubovik, O., Lizcano, G., M'Bainayel, S., Engelstaedter, S., 2007. Mineral dust emission from the Bodélé Depression, northern Chad, during BoDEx 2005. J. Geophys. Res. 112, D06207. doi:10.1029/2006JD007170.

Torres, O., Tanskanen, A., Veihelmann, B., Ahn, C., Braak, R., Bhartia, P.K., Veefkind, P., Levelt, P., 2007. Aerosols and surface UV products from Ozone Monitoring Instrument observations: an overview. J. Geophys. Res. 112, D24S47. doi:10.1029/2007JD008809.

Torres, O., Bhartia, P.K., Herman, J.R., Ahmad, Z., Gleason, J., 1998. Derivation of aerosol properties from satellite measurements of backscattered ultraviolet radiation: theoretical basis. J. Geophys. Res. 103, D14. doi:10.1029/98JD00900.

Torres, O., Bhartia, P.K., Herman, J.R., Sinyuk, A., Ginoux, P., Holben, B., 2002. A long-term record of aerosol optical depth from TOMS observations and comparison to AERONET measurements. J. Atmos. Sci. 59 (3), 398–413. doi:10.1175/1520-0469.

Twomey, S.A., 1977. The influence of pollution on the shortwave albedo of clouds. J. Atmos. Sci. 34, 1149–1152.

Veefkind, J.P., de Leeuw, G., Stammes, P., Koelemeijer, R.B.A., 2000. Regional distribution of aerosol over land, derived from ATSR-2 and GOME. Remote Sens. Environ. 74, 377–386.

Washington, R., Todd, M.C., Engelstaedter, S., Mbainayel, S., Mitchell, F., 2006. Dust and the low-level circulation over the Bodélé Depression, Chad: observations from BoDEx 2005. J. Geophys. Res. 111, D03201. doi:10.1029/2005JD006502.

Webster, P.J., 1987. The elementary monsoon. In: Fein, J.S., Stephens, P. (Eds.), Monsoons. John Wiley & Sons, pp. 3–32 (Chapter 1).

Williams, E.R., 2008. Comment on "Atmospheric controls on the annual cycle of north African dust" by S. Engelstaedter and R. Washington. J. Geophys. Res. 113, D23109. doi:10.1029/2008JD009930.